Pickering Water-in-oil Emulsions Stabilized Solely by Fat Crystals

ADVANCED MATERIALS INTERFACES
Open Access
www.advmatinterfaces.de

Pickering Water-in-Oil Emulsions Stabilized Solely by Fat Crystals

*Elizabeth Tenorio-Garcia, Andrea Araiza-Calahorra, Michael Rappolt, Elena Simone, and Anwesha Sarkar**

Water-in-oil (W/O) emulsions have attracted heightened attention because of the ever-increasing interest in using non-calorific water to replace calorie-dense fat in food. However, designing clean-label and ultra-stable W/O emulsions is a longstanding challenge in colloid science. Herein, a novel, facile approach is introduced to designing cocoa butter (CB)-based crystals to stabilize Pickering W/O emulsions. Results using a combination of small- and wide-angle X-ray scattering and microscopy across length scales reveal that the fat crystals formed in an oleogel of CB with vegetable oil offer high stability to water droplets (up to 60% (v/v)) against coalescence and phase inversion, over storage for 7 months. Such extraordinary stability is attributed to the nanoplatelet-like CB crystals of β_V polymorph located at the water–oil interface and to the inter-droplet fat crystal network formation, interlocking the water droplets. The increment in water volume fraction endows gel-like properties with the water droplets acting as "active fillers." These newly designed Pickering W/O emulsions stabilized solely by fat crystals with unusual rigidity offer great promise for fabricating advanced functional materials in food, pharmaceutics, and cosmetic applications, where long-term stabilization of water droplets using sustainable particles is a necessity.

1. Introduction

Fat crystallization offers a wide range of physicochemical and sensorial properties to fat continuous systems, resulting from the complex interplay of the nanostructure of fat crystals, their spatial arrangement, and the intrinsic microstructure they provide.[1–4] Due to the ever-growing demands of health awareness and growing concerns regarding the sustainability of solid fats, there has been a burgeoning interest in reducing fat content in various food and soft material applications.[5] However, any modifications aimed at reducing fat can have adverse effects on the microstructure, leading to undesirable functional, textural, and mouthfeel properties.[6,7] Oleogel, which is a liquid oil transformed into an anhydrous, viscoelastic, soft material using a gelator, offers an alternative way to not only replace saturated fats but also to provide structure to oils.[8] An oleogel is created by combining an olegelator with a solvent, typically vegetable oils. The nature of the oleogelator can be lipid-based (e.g., monoacylglycerols (MAGs), diacylglycerols (DAGs), triacylglycerols (TAGs), fatty acids, cocoa butter), non-lipid-based (e.g., lecithin, waxes, sorbitan derivatives) or polymeric (e.g., proteins, gums and resins, cellulose derivatives).[9] Oleogelators prevent phase separation by intermolecular forces such as hydrogen bonding and van der Waals, resulting in the formation of a solid self-supporting material that entraps the oil.[10] Although oleogels can contribute to reducing saturated fat, the high caloric content derived from the oil remains a concern.[5]

Water-in-oil (W/O) emulsions, which consist of a fat continuous system with dispersed water droplets, have emerged as promising colloidal templates for reducing large proportions of fat.[5,11] Emulsions are inherently thermodynamically unstable systems due to the immiscibility of their components, which tend to separate into their individual phases without proper stabilization.[11] To enhance stability, surfactants or Pickering particles are commonly added. However, achieving longer-term kinetic stability against coarsening in W/O emulsions using sustainable, environmentally friendly particles remains a longstanding challenge in colloid science community.[12] Pickering particles derived from natural sources have gained significant research attention in the last few years,[5,10,12–17] to replace the classic surfactants, i.e., polyglycerol polyricinoleate (PGPR), E476, commonly used in fat continuous emulsions. Fat crystals have shown to be an excellent candidate in this endeavor, as they can provide stability to a W/O emulsion while also structuring the oil phase effectively, allowing to create the just-right texture via the

E. Tenorio-Garcia, A. Araiza-Calahorra, M. Rappolt, E. Simone, A. Sarkar
Food Colloids and Bioprocessing Group
School of Food Science and Nutrition
University of Leeds
LeedsLS2 9JT, UK
E-mail: a.sarkar@leeds.ac.uk
E. Simone
Department of Applied Science and Technology (DISAT)
Politecnico di Torino
Torino10129, Italy

The ORCID identification number(s) for the author(s) of this article can be found under https://doi.org/10.1002/admi.202300190

DOI: 10.1002/admi.202300190

formation of a crystal network in the continuous phase. Fat crystals can provide stability to emulsions by Pickering mechanism as well as by network stabilization or a combination of both, which depends on the type of fat and the presence of other additives, such as surfactants.[7,10]

In previous work, fat crystal-stabilized W/O emulsions have been successfully prepared by using lipidic surfactants (e.g., glycerol monostearate (GMS) and Glycerol monoleate (GMO)) and waxes (e.g., shellac, candelilla waxes).[10] The type of oleogelator used determines the preferred location of crystallization, either at the water-oil (W-O) interface for Pickering stabilization (*e.g.*, GMS), or through the supramolecular assembly of fat crystals (e.g., hydrogenated canola oil, HCO), or the combination of both phenomena (GMS:HCO and shellac wax).[6,10,18] The oleogel is normally formed following the emulsification step, by dropping the temperature from ≈80 °C to below the melting point of the gelator.[10] Triacylglycerol-based oleogelators have the advantage of having a low melting point, which avoids the need for a high working temperature that can lead to oxidation of the liquid oil. During cooling to the crystallization temperature, the oleogelators preferentially nucleate at the interface, forming an interfacial barrier and a bulk network of crystals that provide exceptional stability against droplet coarsening.[19] Nevertheless, in cases where the surface activity of these lipid gelators is insufficient, emulsifiers need to be added to ensure stability to these emulsions. This is because surfactants can modify the surface properties of crystals; furthermore, surfactants can also inhibit or promote nucleation and crystallization, modifying the size and shape of the crystals formed.[20,19,2]

Cocoa butter (CB) crystals, which are natural and green particles, have been demonstrated to offer stability to air-water interfaces.[8] Their tendency to form oleogels with liquid oils has been reported to be linked to the CB concentration in the liquid oil, and to their chemical composition which is high in saturated lipids (66% saturated fatty acids, of which 24% corresponds to palmitic acid ($C_{16:0}$) and stearic acid ($C_{18:0}$)), but also contains a high concentration of monounsaturated lipids (36% oleic acid ($C_{18:1}$)).[9] CB TAGs can crystallize in six polymorphic forms with the triclinic form V being particularly desirable for achieving the desired texture and stability in chocolate products.[21–23] To achieve such form, it is important to control the crystallization temperature and shearing level.[23] Additionally, minor components such as MAGs, DAGs, free fatty acids, and phospholipids have an effect on CB's polymorphism, crystallization kinetics, and crystal morphology.[24]

While CB crystals have been employed in the production of stable W/O emulsions in previous literature, these emulsions often required the addition of surfactants such as PGPR to aid stabilization.[25,26] Hence, creating emulsifier-free Pickering W/O emulsions solely with fat crystals to offer long-term stability while also providing the necessary rheological properties of the emulsions containing larger volume fractions of water, remains unresolved to date in the literature.

Herein, we fabricated for the first time emulsifier-free W/O emulsions using fat crystals contained in CB and high oleic sunflower oil (HOSO) oleogels as Pickering particles. Results from our study show these fat crystals allowed the stabilization of up to 60% (v/v) water droplets over seven months of storage. This remarkable stability can be attributed to the synergistic effects of both the Pickering effect and bulk stabilization offered by the stabilizing properties of the fat crystals. Notably, the water droplets stabilized by such CB crystals act as "active fillers" contributing to increase viscosity in the system as compared to oleogels without water droplets. These findings present a novel approach for utilizing fat crystals oleogels without the need for additional additives, offering potential for the development of low-calorie, clean-level, and sustainable fat-based systems for various applications in the food industry and allied soft matter applications.

2. Results and Discussion

2.1. Crystallization and Characteristics of Fat Crystals Generated in Oleogels

First, it is important to understand the crystallization behavior and characteristics of the fat crystals formed before utilizing them for stabilizing water droplets. The solid fat content (SFC) plays a decisive role in determining the properties of the resulting CB dispersed in high oleic sunflower oil (HOSO) oleogel i.e. CB + HOSO oleogel (CBolg) containing various volume fractions of CB (10, 15, and 20% (v/v)). This, in turn, affects the ability of the resulting fat crystals to stabilize water-in-oil (W/O) emulsions. The literature has reported that the SFC of 15% CBolg, denoted as 15CBolg, is zero in the temperature range of 25 to 45 °C,[27] indicating that no crystals will remain to act as Pickering particles at such high temperatures. The SFC (%) values of the oleogels used in this study can be estimated by interpolation using a Gompertz-type equation:[28]

$$SFC\ (\%)\ (T, CB) = \left(b_0 + b_1 CB\right) e^{-e^{\frac{-(T-(b_{01}+(b_{11}CB)))}{c}}} \quad (1)$$

where T is the sample temperature in °C, CB is the % concentration (v/v) of added CB, and the coefficients $b_0 = 1.24$, $b_1 = 73$, $b_{01} = 13.48$, $b_{11} = 38.5$ and $c = -4.66$ are determined via previous interpolation of data from the same oleogel system.[27] Making the corresponding calculations, for the temperature used in this work (23 °C), the SFC of 10CBolg was determined to be 0.22%, which appeared to be too low for stabilizing W/O emulsion. In contrast, the SFCs values for 15 and 20CBolg, the latter containing 20% (v/v) CB, were calculated to be 1.35 and 2.71%, respectively. Noteworthy, the calculated SFC value obtained for 20CBolg should be taken with caution as the validity of Equation (1) is limited to CB concentrations ranging from 9 to 15% (wt).

The formation and structure of fat crystals are influenced by several parameters, including cooling rate, crystallization temperature, and shear.[29] TAGs undergo crystallization by initially forming nuclei, which then developed into lamellae and subsequently assemble into nanoplatelets. These nanoplatelets randomly aggregate to form characteristics agglomerates, such as spherulites.[30] To determine the optimal composition of fat crystals for stable W/O emulsions design, two different tempering temperatures (17 and 23 °C) and storage times (0.5–4 days) were used to monitor the evolution of the number, shape, and size of crystals in CBolgs containing 10%, 15%, and 20% (v/v) CB in HOSO. Optical polarized light microscopy (PLM) was employed to capture images of the structure of the CB crystals' structure under the specified conditions, as shown in **Figure 1**.

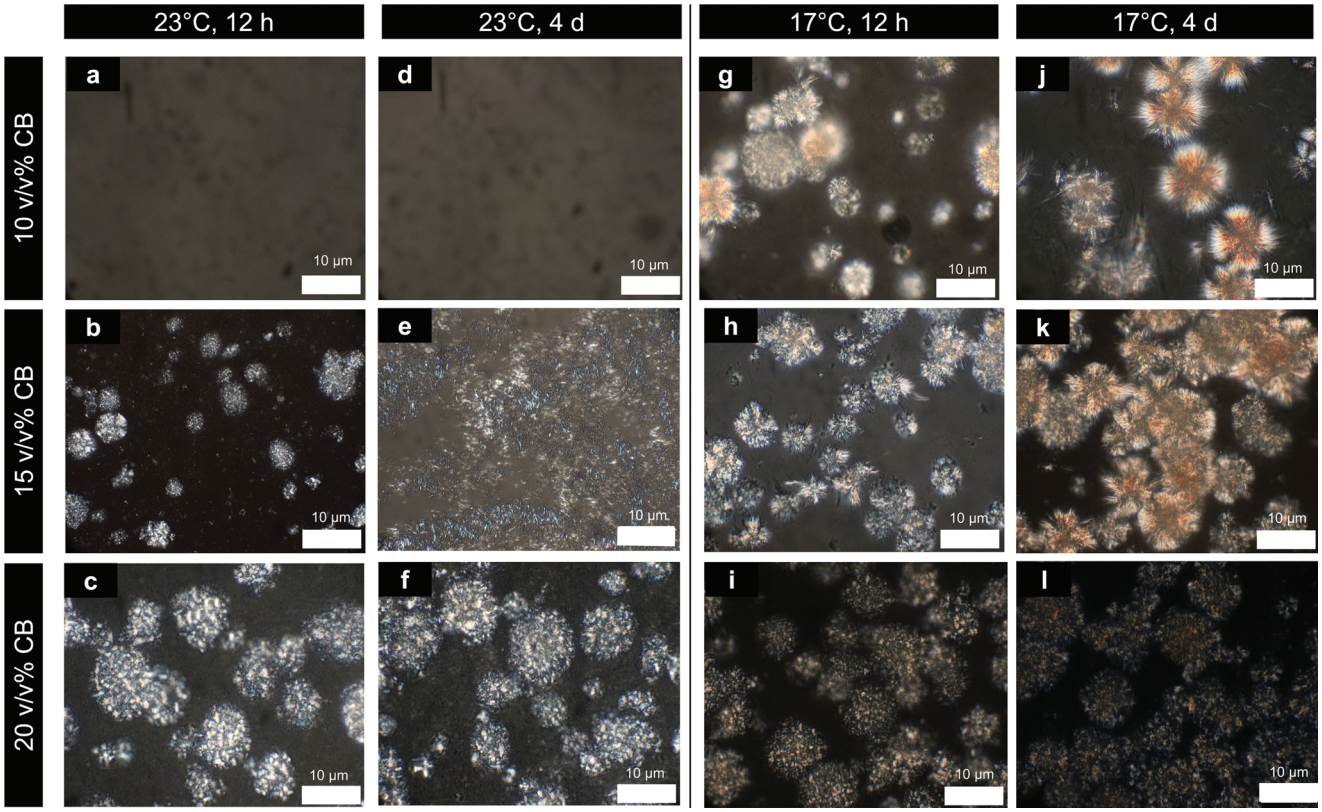

Figure 1. Polarized light micrographs of fat crystals. The influence of the concentration of CB crystal structuring in high oleic sunflower oil (HOSO) oleogel is shown in (a–c) for 10%, 15%, and 20% (v/v) CB, respectively, after the crystallization process with tempering at 23 °C, followed by maintaining the same temperature for 12 h (see Figure S1, Supporting Information). The evolution of CB crystal morphology after 4 days for the three aforementioned concentrations is shown in (d–f). The effect of the final tempering temperature on the morphology of the CB crystals was investigated by changing the temperature to 17 °C for the three concentrations (g–i) followed by their evolution over 4 days of storage period (j–l).

The crystallization process was monitored in real-time using light transmittance values (Figure S1a–d, Supporting Information). A sudden reduction in transmittance indicated the commencement of crystal formation at the crystallization temperature (T_c). As expected, T_c was directly proportional to the concentrations of CB. The 20CBolg had the highest T_c at 8.53 ±1.94 °C (Figure S1c, Supporting Information), followed by 15CBolg (Figure S1b, Supporting Information) and 10CBolg (Figure S1a, Supporting Information) with T_c values of 7.19 ±1.18 °C and 5.84 ± 0.53 °C, respectively. Considering the gel-like architecture of the oleogels, a tempering temperature of 23 °C was chosen to closely resemble room temperature conditions, which would facilitate potential industrial-scale applications. It is important to note that higher temperatures would cause the fat crystals to melt, as the CB oleogel's melting point is 25 °C. At 23 °C, the resulting 15CBolg exhibited a more fluid-like behavior, due to the low solid fat content but preserved some CB crystals to stabilize W/O emulsions.

Irrespective of their conditions, the CB crystals in 15CBolgs and 20CBolgs displayed the characteristic spherulite-like morphology of CB (Figure 1), which has been observed previously in literature in CB dispersions, native CB and chocolate formulations.[23,24,22,31] Of more importance, as the CB content increased, CBolg showed a limited number of small isolated crystals (Figure 1f), whilst 20CBolgs (Figure 1c) showed a rather uniform distribution of CB spherulites with a diameter of approximately 10 µm at 23 °C within 12 h. The interplay between temperature and storage time allowed for altering the quantity and size of the CB crystal aggregates. For instance, although a limited number of crystals were observed at the lower concentration of CB (10% v/v) even after 4 days storage at 23 °C (Figure 1d), larger CB crystal agglomerates with diameters higher >15–20 µm appeared after 12 h at 17 °C (Figure 1g). Transmittance values of 10CBolg at 17 °C showed a remarkable decrease to 25.32% (Figure S1d, Supporting Information), even higher than that of 15CBolg at 23 °C (Figure S1b). Further growth of the CB crystals is observed during the 4 days of storage (Figure 1j).

Meanwhile, 15CBolg behaved slightly differently as the CB agglomerates appeared to decrease in size after 4 days of storage at 23 °C (Figure 1e), but their number increased and demonstrated continuous network unlike the other time points. Although this was repeatable results, one should take such data with caution as CB crystals may take significantly longer time to reach equilibrium under static conditions for pure CB,[23] which may alter by shearing.[32] In addition, blend of lipids such as the case in this study might affect crystallization equilibrium and consequently crystal structure as a function f time.[33] Thus, more detailed research should be done to understand this behavior, which is out of the scope of this investigation. The transmittance value (Figure S1e, Supporting Information) dropped in

magnitude from 72.05% to 51.73% after 4 days of storage at 23 °C. However, the CB crystallization behavior in 15CBolg (Figure 1h,k) was similar to that in 10CBolg (Figure 1g,j) at 17 °C. Particularly, a remarkable feather-like appearance[22] of the spherulites was observed at longer storage times (4 days) at 17 °C in both 10CBolg and 15CBolg (Figure 1j,k), with more overlapping crystals in 15CBolg.

Noteworthy, neither storage time nor temperature seems to affect the structure of 20CBolg (Figure 1f,i,l), as it displayed similar-sized CB agglomerates throughout the experimental window (Figure 1c). This CB concentration had the highest undercooling at 23 °C, reaching the equilibrium earlier, and Ostwald ripening was less evident due to its high SFC. Previous studies have shown that diluting CB in vegetable oils (e.g., soybean, canola oil, and HOSO) decreases the melting point of the formed solid crystals due to the molecular interactions of their TAGs contained in the oil.[8,31] The melting point under the experimental conditions tested in this work also presented a reduction from 36.7 °C of pure CB to around 29 ± 0.7 and 29.3 ± 0.6 °C for the 15 and 20CBolg, respectively (see differential calorimetry (DSC) thermograms in Figure S2, Supporting Information). This suggests that the fat crystals formed in the oleogels are probably not pure CB crystals, which will be further discussed in the section involving scattering data. However, for convenience, the term "CB crystals" will be used henceforth to refer to the fat crystals used to stabilize W/O emulsions.

2.2. Microstructure and Stability of CB Crystals-stabilized Pickering W/O Emulsions

The CB crystals obtained after 12 h at 23 °C were tested for their ability to form and stabilize particle-laden W/O emulsions (**Figure 2**). Transmittance results (Figure S1a, Supporting Information) and PLM micrographs (Figure 1a,d) indicated that no visible crystal remained in the 10CBolg, which is in line with the small SFC value of 0.22%. As expected, unstable W/O emulsions were formed using these oleogels, as indicated by the visual instability observed in the resulting emulsion (Figure 2b). The emulsion presented two distinct colors, with the upper part appearing light yellow, which was characterized by the presence of bigger droplets. This distinction is highlighted by the red arrow in Figure 2b. The droplet size distribution (Figure 2a) of these freshly prepared emulsions with 10% (v/v) CB crystals showed polydispersity, with a predominance of small droplets (positive skewness, 3.55), but also with some larger droplets of sizes between 2 and 5 μm (high kurtosis, 20.39). The mean of the droplet size distribution was 0.504 μm (the value reported is Q2, also known as the second quartile or median, as the distribution was not normal).

Stable W/O emulsions were formed using 15% and 20% (v/v) CB crystals, which showed resistance against visual creaming, coalescence and phase separation (Figure 2c–f). Despite the tendency of CB crystals to form agglomerates in the oleogels, showing large sizes of ≈5–15 μm (Figure 1), small water droplets could be incorporated with the homogenization process indicating that the crystal agglomerates can be broken up into smaller sizes during the emulsification process, allowing the smaller crystals to stabilize the water droplets. To confirm this, the CB crystals were subjected to the same emulsification while maintaining the vessel at 4 °C. It was observed that the intense shearing and turbulence during homogenization led to the broke up of the majority of the agglomerated spherulites into smaller crystals, which were available to stabilize the water-oil interface (Figure S3, Supporting Information). A similar effect was observed during the whipping of the same oleogel, where CB agglomerates were also broken, allowing the stabilization of foams.[8]

Interestingly, the droplet size was significantly different for W/O emulsions stabilized with 15% (v/v) CB crystals ($p < 0.05$), showing a mean droplet diameter of 0.381 μm, whist for 20% (v/v) CB crystals was 0.421 μm suggesting that 15% (v/v) CB crystals were definitely sufficient to create a stable water droplet. However, one may question the increase in droplet size of the emulsions with increased concentration of CB. Briefly, in the absence of buoyancy and inertia effects, the droplet behavior is governed by two dimensionless numbers:[34] The capillary number *Ca* is $Ca = r\eta_c\dot{\gamma}/\sigma$, where η_c is the continuous phase viscosity, *r* the droplet radius, $\dot{\gamma}$ the shear rate, and σ the interfacial tension) and the viscosity ratio λ ($\lambda = \eta_d/\eta_c$, with η_d is the dispersed phase viscosity). For *Ca* larger than a critical value, droplets become unstable and the corresponding *Ca* is known as the critical number Ca_c.[35] The relationship between Ca_c and the deformation of droplets in Newtonian fluids has been investigated by Grace[36] and subsequently by Brujin.[37] They found that the breakup of droplets generally occurs with $\lambda < 3.5$ and $Ca_c > 0.5$. Such breakup of droplets also occur in non-Newtonian fluids.[38] However, for higher viscosities λ or smaller *Ca*, such break up rarely occur. Since 20CBolg had a higher SFC, its viscosity was also higher (more discussed later), giving the crystals a more solid-like behavior as compared to 10CB and 15CB, resulting in limited breakdown during homogenization and formation of bigger Pickering droplets formed using bigger sized crystals.

Since the concentration of 15% (v/v) CB crystals in HOSO was found to effectively stabilize W/O emulsions, this concentration of CB was used to further investigate the amount of water that could be stabilized in a structured W/O emulsion. Findings have shown that 15% (v/v) CB crystals were able of entrapping up to 60% (v/v) water while maintaining kinetic stability (**Figure 3**f–i). The droplet size distribution for the four emulsions containing 30–60% (v/v) water showed similar distribution, with no significant differences ($p < 0.05$) in terms of their mean droplet size, which was ≈0.35 μm (Figure 3a). However, W/O emulsions with 60% of water presented a small portion of bigger droplets, ranging from 1.16 to 4.9 μm (Figure 3a), and with a structure that shows a high quantity of water droplets dispersed between the continuous phase (Figure 3e). The physical appearance of the freshly prepared W/O emulsions is presented in Figure 3f–i, showing not only stability against coalescence but also fluid-like behavior for values of water of 30% (v/v) (Figure 3f). Whereas 40–60% water incorporation presented a more gel-like behavior (Figure 3g–i), indicating that water droplets were acting as "active fillers" in the fat continuous emulsion. Further discussion on this phenomenon can be found in the rheology section.

In the optical micrographs of the four studied emulsions could be appreciated that similar size droplets can be stabilized by the 15% (v/v) CB crystals, regardless of the entrapped water content (Figure 3b–e). Thus, a sufficient number of crystals were present to stabilize and maintain consistent droplet size, while the

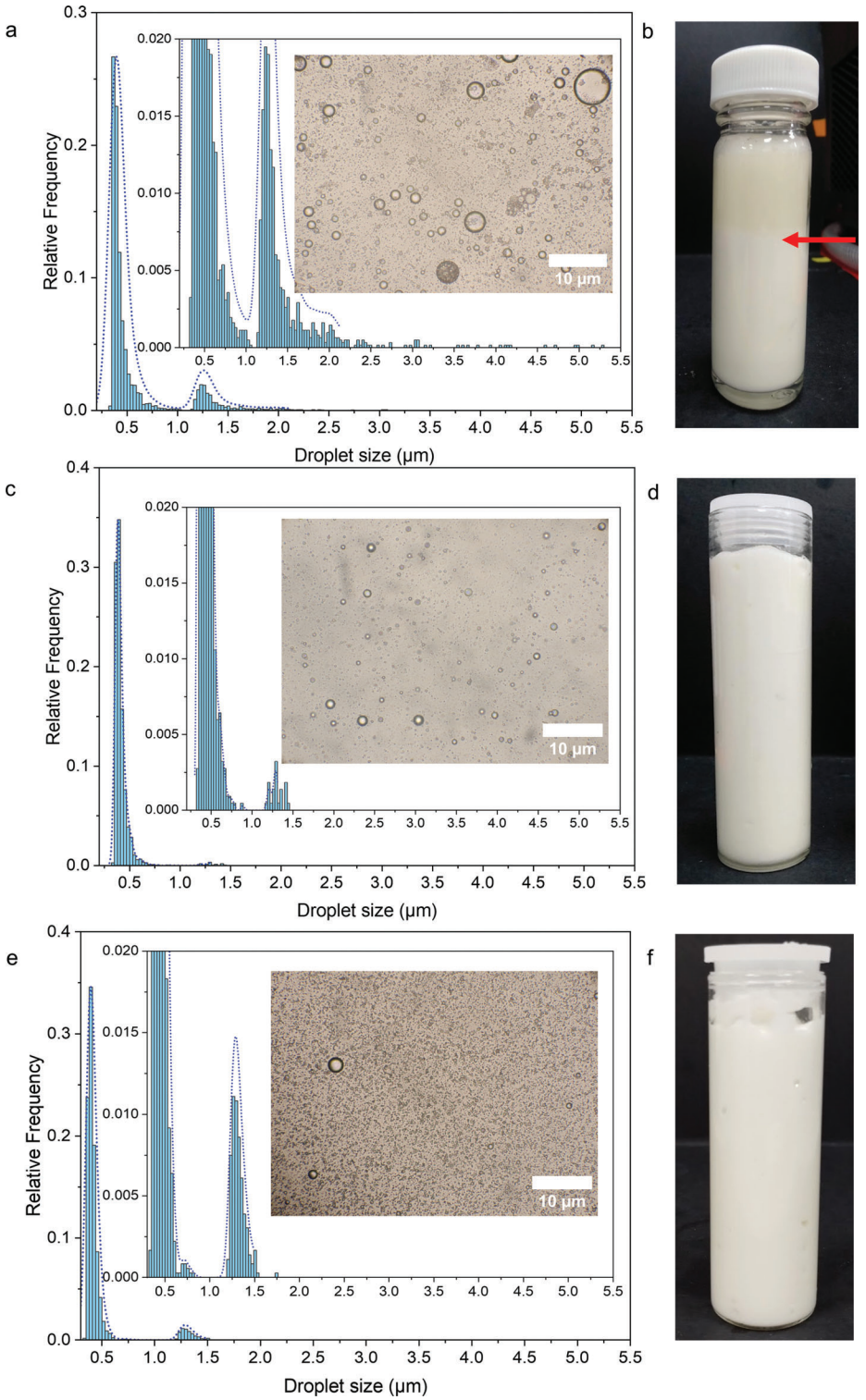

Figure 2. Microstructure of W/O emulsions stabilized with different CB concentrations. As the percentage of CB is related to the amount of CB crystals that can form, three different concentrations of fat crystals (10, 15 and 20% (v/v) CB) were used to evaluate their stabilization properties. The droplet size distribution for the three W/O emulsions stabilized by the aforementioned CB concentrations is shown in (a), (c), and (e). The distributions showed high counts for small droplets; thus a zoom is shown to observe the droplet distribution for larger diameters in each sample (a, c, and e). The optical images show the dilution of the water droplets dispersed in the HOSO (a, c, and e). The W/O was diluted in HOSO + PGPR to obtain a representative distribution and heated to melt the CB crystals before size measurement using image analysis using Matlab. The visual image of the freshly prepared W/O emulsions showing kinetic stability is shown in (b), (d), and (f). The red arrow indicates the instability of the emulsions with 10% CB. The data shows the means of three measurements on triplicate samples ($n = 3 \times 3$).

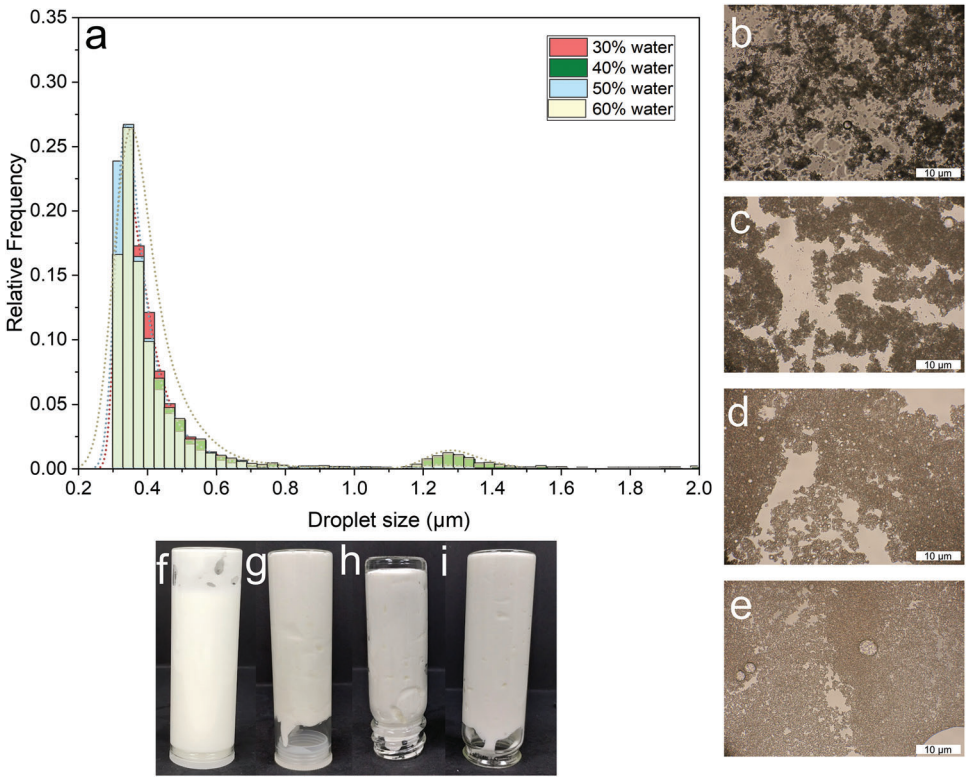

Figure 3. Droplet size distribution and microstructure of W/O emulsions containing increased volume fractions of water droplets. The emulsions were stabilized with fat crystals with 15% (v/v) CB. The capability of the CB crystal to stabilize water droplets was evaluated by using different water concentrations (30–60% (v/v)). The histograms (a) obtained for the droplet distribution of freshly prepared emulsions were fitted by using a 3-parameter lognormal distribution. The microstructure of the emulsions for 30 (b), 40 (c), 50 (d), and 60 (e) % (v/v) of water are shown without doing any dilution, in order to show the aggregation behavior of the water droplets when they are stabilized solely by fat crystals. Images (f–i) show the physical macroscopic appearance and fluid-like properties of the W/O emulsions after a few minutes of preparation. The data show the means of three measurements on triplicate samples ($n = 3 \times 3$).

number of droplets increased as the water content in the emulsion 30–50% (v/v). A possible stabilization mechanism can be associated with the CB crystals wetting the water phase during the emulsification process, allowing the previously formed CB crystals in the oleogels to migrate to the water-oil interface. In addition, the shear provided by the emulsification process combined with the cold dispersed phase (4 °C) facilitates the formation of new crystals that aggregate at the interface. The aggregation of these smaller crystals forms a solid shell around the droplets during and immediately after the emulsification.[39] The maintenance of temperature at around 20 °C during the homogenization process was essential to prevent the melting of CB crystals under high shear conditions.

The W/O emulsions stabilized solely by CB crystals can be clearly appreciated in the confocal laser scanning microscopy (CLSM) images (**Figure 4**a–d). The results clearly demonstrated that CB crystals clearly acted as Pickering particles, providing stabilization to the water droplets in the emulsions, without any added surfactant or additive. The CB crystals stabilize the emulsions by two possible mechanisms: 1) Pickering stabilization by particles that coat the water-oil interface, wetted partially by the oil and water phases, and 2) network stabilization within the bulk of the liquid oil through the aggregation of fat crystals, preventing coalescence of the water droplets.[11,2,8,40] From these results an important question might be which of the two mechanisms dominated in Pickering stabilization of these water droplets stabilized by CB crystals. The CLSM images reveal that the needle-like CB crystals (at a mesoscale) cover the water droplets through interfacial coverage, while the formation of a network of crystals between the water droplets via crystalline bridges in the continuous phase is also evident (white arrows in Figure 4a). Despite the low SFC calculated for the 15CBolg, there are sufficient CB crystals to stabilize 30–60% (v/v) water in the emulsions (Figure 4a–d). It is important to note, that the emulsification process, along with the use of cold water, may have promoted the formation of new crystals via secondary or primary nucleation, thus increasing the SFC. However, when the emulsions are stored at 23 °C, they reach an equilibrium state consistent with the initial state SFC of the oleogel at that temperature. For the emulsion with higher water content (40%, 50%, and 60% (v/v), CB crystals formed a relatively thin layer of crystals around water droplets and some of the neighboring droplets appeared to be sharing the same crystals (Figure 4b–d), highlighting that bulk stabilization might be essential to offer longer term kinetic stability to these Pickering emulsions. Evaluating the behavior of fats is a challenging task due to the various levels of organization of fats present in the solid phase, such as lipid composition of crystals, and the interaction of the solid crystals with the liquid water phase (to be

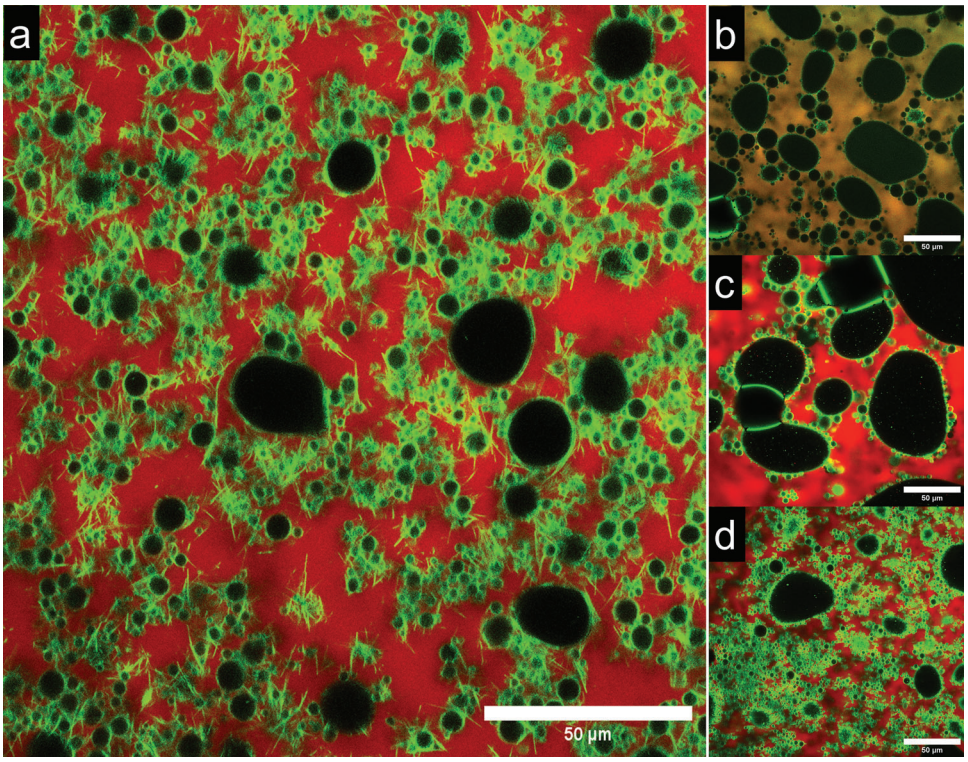

Figure 4. Confocal micrographs of Pickering W/O emulsions stabilized solely by fat crystals. CB crystals at the interface of freshly prepared W/O emulsions containing different volume fractions of water can be observed. The emulsions were fluorescently dyed with a blend of Nile Red and Nile Blue stains in order to differentiate the CB crystals from the bulk oil phase (HOSO). By chemical preference, the Nile Blue goes to the surface of CB crystals (green) while Nile red stains the HOSO (red). Long needle-like fat crystals can be appreciated for the W/O emulsions with 30% v/v of water (a), while at higher volume fractions of water (40 (b); 50 (c); and 60% (d) (v/v)), smaller crystals surrounding the water droplets are observed (b, c, d). The white arrows in (a) show fat crystal networking in the bulk phase forming fat crystal-fat crystal aggregate further contributing to droplet stability in addition to the aforementioned interfacial stabilization.

discussed later).[41] While confocal images allow observing the aggregation of several crystallites at the W-O interface, cryogenic scanning elcetron microscopy (cryoSEM) provides better resolution enabling a better appreciation of the geometry of the crystals at the mesoscale. To understand the morphology of the CB crystals, **Figure 5**a,b shows the cryoSEM images which confirm the presence of CB crystals, as observed by the nanoplatelets surrounding the water droplets (yellow arrow). In addition, some nanoplatelets can be seen positioned between the droplets and the continuous phase, which may contribute to network stabilization (red arrows), consistent with the CLSM images (Figure 4a–d). Nevertheless, one should be cautious in using the cryoSEM images as the preparation procedure of freeze-fracture might impact the crystallization behavior of the fat crystals both in at the droplet interface as well as in the bulk phase.

At an angstrom scale, crystals can adopt one of the three main polymorphic forms for triacylglycerols (α, β', and β), which depends on the crystallization behavior. In addition, the polymorphic structure of the Pickering CB crystals can evolve over time. Therefore, it is important to ask whether the polymorphic structure of the Pickering CB crystals at the W/O emulsions are similar to those that were generated during the oleogel formation. Studies have shown that higher stability and melting points are achieved for β V and VI forms for CB crystals,[42] which are related to the molecular arrangement of the main TAGs of CB in a 3D-triclinic solid crystal. Small- and wide-angle X-ray scattering (SAXS and WAXS) was conducted to determine the polymorphic structure of the oleogel and the corresponding W/O emulsions (**Figure 6**a). The 20CBolg display reflections corresponding to the short-spacing of 0.460, 0.390, and 0.368 nm^{-1} (Figure 6c). These reflections define the crystalline 2D-oblique sub-cell[43] and relate to the chain packing in β V polymorphic form, in which the diffraction peak at $2\pi/0.460$ nm^{-1} is most intense[44] (see detailed calculation of chain packing in Theory S1 and associated schematic Figure S4, Supporting Information). The lamellar 3L-stacking corresponds to a long *d*-spacing of 6.74 nm (Figure 6b). Previous studies have demonstrated that the polymorphic structure obtained is the β V[8] under similar conditions of treatment of CB at different concentrations, and there is no transformation to the VI polymorph over months of storage.

The CB crystals in the W/O emulsion display similar values for the dominant long (6.76 nm) and short (0.460 nm) spacing, but with a weaker signal-to-noise ratio; we note, the weaker diffraction peaks in the WAXS regime could not be resolved (Figure 6d,e). Nevertheless, the β V polymorphic crystals are confirmed, stabilizing the water-oil interface, as CB-based oleogels with the same crystallization process.[8] However, comparing the data given on the co-crystallized CB in this study to pure CB crystals measured in our lab under the same isothermal conditions

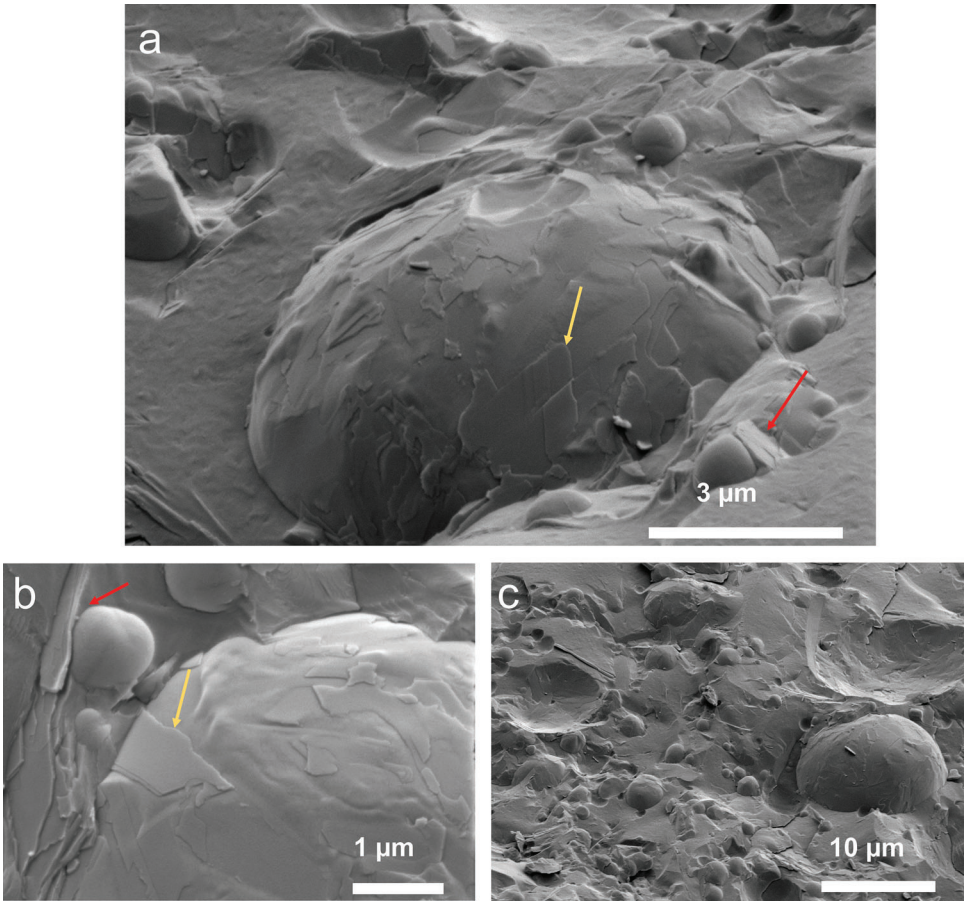

Figure 5. Morphology of the fat crystal in a W/O emulsion. The cryogenic scanning electron microscopy (cryoSEM) images show the morphology of a W/O emulsion (30% (v/v) water) stabilized by fat crystals after 1 day of preparation and storage at 23 °C. The crystals appear as nanoplatelets and seem to be located both at the surface of the water droplets and also in the continuous oil phase, as shown in (a) and (b), which are marked in the image by the yellow and red arrows, respectively. Low magnification (c) of the emulsion microstructure shows a wider image with numerous water droplets and CB nanoplatelets in the system.

(data not shown, but displaying very similar diffraction patterns), we observed an overall lower density in co-crystallized CB. This can be judged both, from the long as well as short spacings. First, the stacking repeat in co-crystallized CB of 6.74 nm compares to 6.49 nm in pure CB; that is, as a lower density of the β V polymorphic crystals is reflected in a relatively smaller chain tilt, the recorded bigger *d*-spacings in this work confirm the up-take of TAGs from the HOSO phase. Second, we did determine from the wide-angle data the area per chain in both, the co-crystallized CB and pure CB. In the latter, the short spacings of the (10), (11) and (−11) reflections are 0.457, 0.387, and 0.367 nm^{-1}, which compare to the values given above and Figure 6c. In turn, this leads to an area per chain of 0.189 nm^2 for pure CB, which compare to a bigger area per chain in co-crystallized CB of 0.192 nm^2. Overall, the chain packing density changes are not big, but still significant. While the crystal form is identical to pure CB, CB in HOSO oleogels display a slightly lower TAG packing density, and thus explain their lower melting profile. Furthermore, most likely the HOSO improves the wettability of the CB crystals to diffuse to the water-oil interface. Since there are saturated fatty acids such as palmitic acids, stearic acids which are common between CB and HOSO. Even if the percentages are significantly less in the latter (<8%),[45] it remains difficult to pinpoint the exact influence of HOSO TAGS versus CB TAGS in the fat crystals stabilizing the droplets, which needs further work beyond this study.

2.3. Storage Stability of the W/O Emulsions with Different Water Content

Besides microstructural evidence, it is important to understand the influence of storage on droplet size evolution for Pickering stabilization. **Figure 7**e–j shows that the emulsions had a polydisperse distribution of droplets for emulsions storage for one month. A weak gel-like behavior that showed visual resistance to flow is shown in Figure 7a–d. Although the droplet size was relatively small, the mean droplet size evolved slightly from week 0 to week 1 from ≈0.37 µm to ≈0.42 µm ($p > 0.05$) irrespective of water volume fractions (Figure 7l-l). From week 1 to week 4, the droplet size distribution remained fairly constant ($p > 0.05$). A few droplets with diameter ranging between 1.6 and 5.9 µm (Figure 7e) appeared as a function of storage. This increment is more noticeable in W/O emulsions with 60% (v/v) of water (Figure 7e); however, such small increments did not appear to

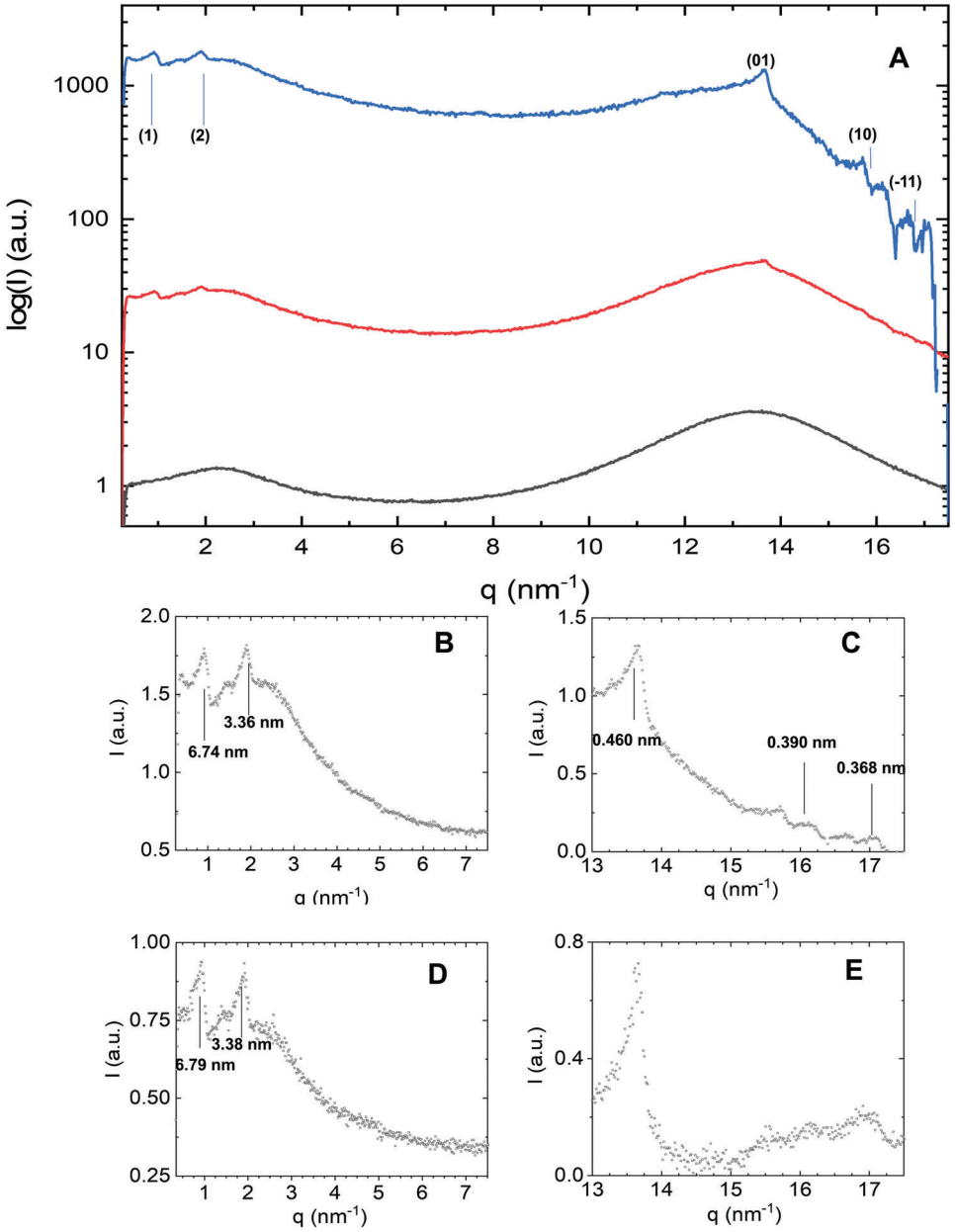

Figure 6. X-ray scattering patterns of oleogels and W/O emulsions. The scattering curve (a) of I_{HOSO} (black), oleogel $I_{HOSO+CB}$ (red) as well as the solid crystals contribution ($I_{HOSO+CB}-I_{HOSO}$) (blue) are presented. The first two Miller indexes (1) and (2) are associated with the 3L-stacking of the β-polymorph of CB and their lattice spacings are given in (b). The β-polymorph of CB is maintained for the W/O emulsion similar to that in the oleogels (e). Short-spacing diffraction peaks associated with the packing of the hydrocarbon chains are shown in (c) and (e) for the CB/HOSO oleogel and the W/O emulsion stabilized by fat crystals, respectively. The Miller indices of the monoclinic sub-cell are given in (a). The oleogels used contain 20% (v/v) of cocoa butter (CB) in high oleic sunflower oil (HOSO) (20CBolg) and the emulsions containing 30% (v/v) water containing 20% (v/v) CB crystals.

have an effect on the physical stability and average droplet size of the emulsions as a function of storage ($p < 0.05$) (Figure 7k,m). Even after a storage period of seven months, the emulsions exhibited limited increase with an average droplet size of 0.86 μm observed for both the 50 and 60% water emulsions (Figure 7m). Of more importance, the emulsions exhibited remarkable physical stability as evidenced by the absence of phase separation (Figure 7k,l). This stability can be attributed to the combined effect of Pickering and bulk stabilization provided by the 15% (v/v) CB crystals. The presence of these crystals appears to have played a crucial role in maintaining the emulsions' kinetic stability over an extended period. Such extraordinary stability has been previously observed in foams (stabilized with CB + HOSO-based oleogel) stored at room temperature over fifteen months by tomographic analysis.[46] Optical micrographs of the W/O emulsions with 30–60% (v/v) of water (Figure 7n–q) further confirm that small droplets still persisted after seven months although there were few larger droplets. Figure 7k depicts the gel structure of

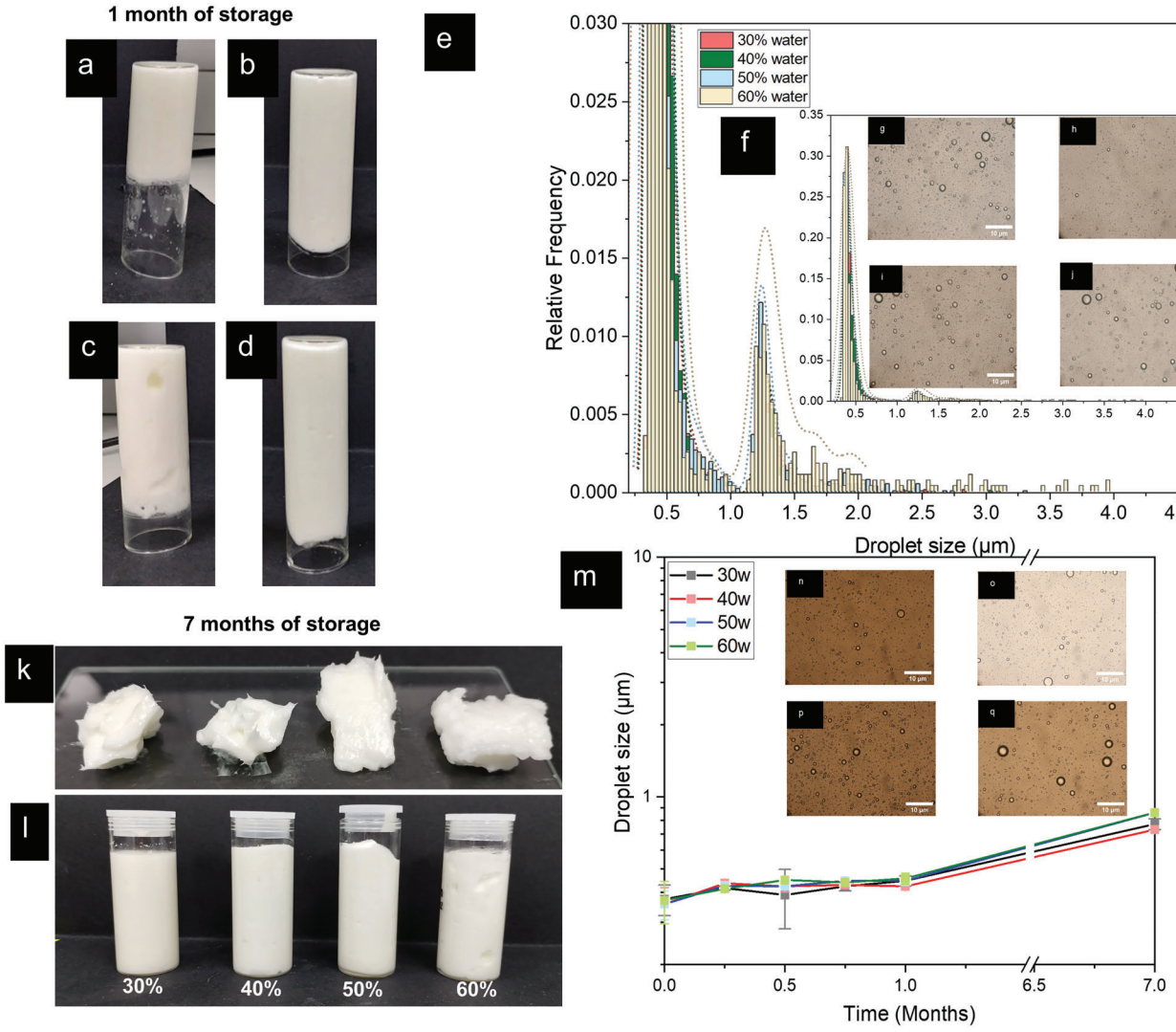

Figure 7. Evolution of the emulsion microstructure with different water contents over time and their physical stability. Visual images of W/O emulsions for 30%, 40%, 50%, and 60% (v/v) of water, (a-d) respectively, storage at 23 °C for 4 weeks. The bottles containing the emulsion were put in an inverted position to highlight the solid-like behavior of the different samples after 1 month of storage. Droplet size distribution is shown for low frequency to highlight the counts of higher droplets (e). The complete distributions showing the high frequency of small droplets after one month are shown in (f). The micrographs depict the change in the microstructure of the W/O emulsions containing 30 (g), 40 (h), 50 (i), and 60 (j) % (v/v) of water during one month of storage. The physical stability and the appearance of emulsions stored at 23 °C during seven months is shown in k and l, respectively. The droplet size change over time is shown in graph (m) for the different water content over 7 months, while the microstructure is shown in the micrographs in (n–q). The graph plots the fitted means which were obtained by a General linear model ($p < 0.05$).

the emulsions after seven months of storage, for the various water content compositions.

After a long period of storage at 23 °C, the increment in the size of the CB crystals was evident in CLSM images, small crystals appeared to fuse and recrystallize on the surface of the large crystals, leading to a thickening/ networking of the crystals both in the bulk and at the water/oil interface[41] (**Figure 8**). The crystal size increment at constant temperature may be attributed to Ostwald ripening, also known as aging of the crystals. The crystals forming a layer around water droplets appeared to be thicker (Figure 8a–c) than in the freshly prepared emulsion at water contents of 30, 40, and 50% (v/v) (Figure 4a–c). In the emulsions stabilized by fat crystals, the structure will be determined not only by the water droplets but also by the crystal network of the oleogels, as the water droplets will be trapped within the CB crystal network. As can be seen in the CLSM images, the CB crystals are also structuring the emulsion, as their size is larger after a month (Figure 8a–c). The higher the water content, the more water droplets are structuring the emulsion, leaving less space for CB crystals to grow via Ostwald ripening. Emulsions with 50% of water showed a high packing of water droplets (Figure 8c). These emulsions presented a noticeable crystalline network around the water droplets, with a high amount of CB crystals in the bulk oil. Emulsions with 60% (v/v) of water require a high amount of CB crystals to stabilize the droplets and the available ones were just enough to coat the droplets for freshly prepared

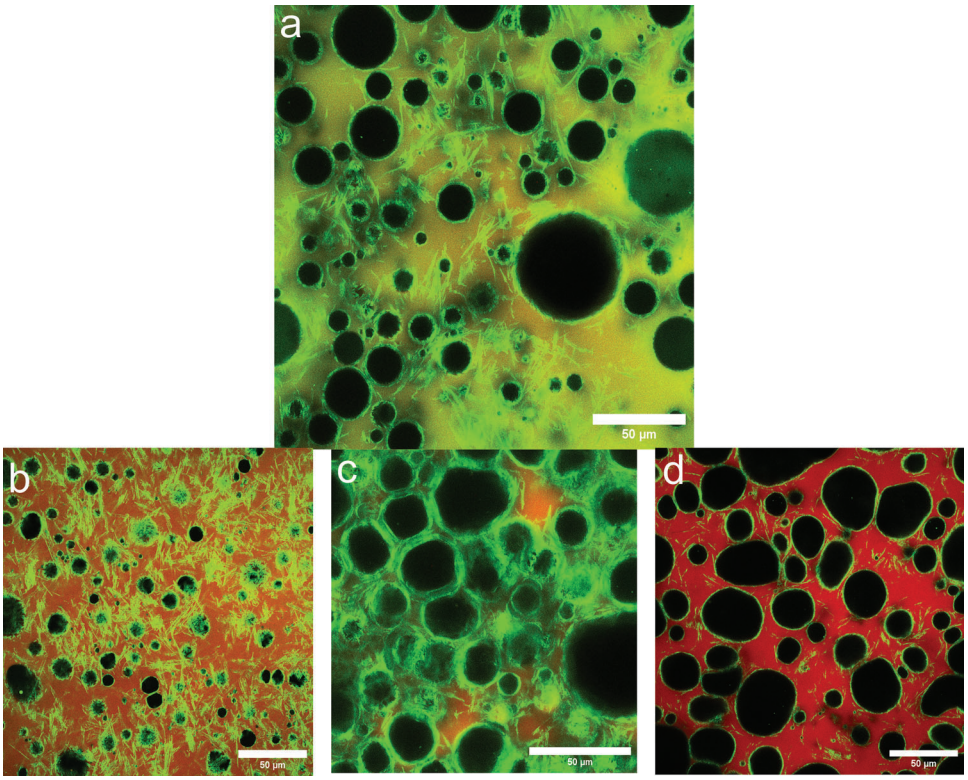

Figure 8. Confocal microstructure of emulsions after storage for a month. Evolution of the droplet structure and the arrangement of CB crystals in the W/O emulsions with various water volume fractions (30 (a), 40 (b); 50 (c), and 60% (d) of water (v/v), respectively) stored at 23 °C for 1 month. The emulsions were fluorescently dyed with a blend of Nile Red and Nile Blue stains in order to differentiate the CB crystals from the bulk oil phase (HOSO). By chemical preference, the Nile Blue goes to the surface of CB crystals (green) while Nile Red stains the HOSO (red). Long needle-like fat crystals continue to dominate the interface of W/O emulsions with 30% v/v of water even after a month of storage (a). The needle shape of CB crystals is evident for all samples after a month of storage.

emulsions (Figure 4d). Thus, as one might expect, Ostwald ripening of the crystals in the bulk phase of emulsions with such a high amount was not significant after one month of storage (Figure 8d).

2.4. Rheological Performance of Pickering W/O Emulsions

The mechanical performance of fat continuous emulsions is linked to their microstructure, composition, and interactions within their components (droplets, fat crystals, emulsifiers, fat networks, and so on).[47] The rheological properties of oleogels are determined by the properties of the CB crystals (size, shape, and polymorphism), the crystal aggregates as well as the SFC.[29] Often replacing fat by adding water can soften a fat continuous material, due to the much lower rigidity of the entrapped water droplets as compared to the CB crystal network.[26] Hence, it was important to understand how the addition of 30–60% (v/v) of water can influence the rheological performance of a 15% v/v CB oleogel. **Figure 9**a shows the apparent viscosity of the 15CBolg and the corresponding W/O emulsions containing different volume fractions of water droplets. Both the 15CBolg and the W/O emulsions presented a typical shear-thinning behavior, as seen previously for W/O Pickering emulsions stabilized by other particles.[48] As one might expect, at high-volume fractions of water, the dense packing of the droplets increases their aggregation and consequently the apparent viscosity, which tends to break in the direction of the flow.

At low shear rates (<10 s^{-1}), the apparent viscosity of the emulsions with 60% (v/v) of water content (i.e., volume fraction $\Phi >$ 0.5) increases by an order of magnitude compared to the 15CBolg (Figure 9a). Also, the addition of water showed a dose-dependent behavior from 30 to 50% (v/v) increasing the apparent viscosities at low shear rates. This suggests that there is a strong interaction between the water droplets and the fat crystals.[3] The CB crystals located at the surface of the emulsion droplets were strongly linked within the continuous phase and reinforced the crystal network, as seen in the CLSM images (Figure 4). W/O emulsions stabilized with PGPR are a clear example of a weak interaction between the droplets, as their viscosity for 30% of water is typical of a Newtonian fluid, with much lower viscosity values (238 s^{-1}) as compared to both the 15CBolg and all the studied emulsions (Figure S5a, Supporting Information). However, the viscosities of the emulsions and CBolg at high shear rates (>100 s^{-1}) were close to each other. Droplets with attractive interaction tend to form aggregates due to van der Waals' forces; however, these aggregates are elastic and can be deformed when a high shear rate is applied. If the shear rate is strong enough to break such aggregates, the droplets may align in the direction of the flow, with a subsequent decrease in the apparent viscosity.[47,49] In the case

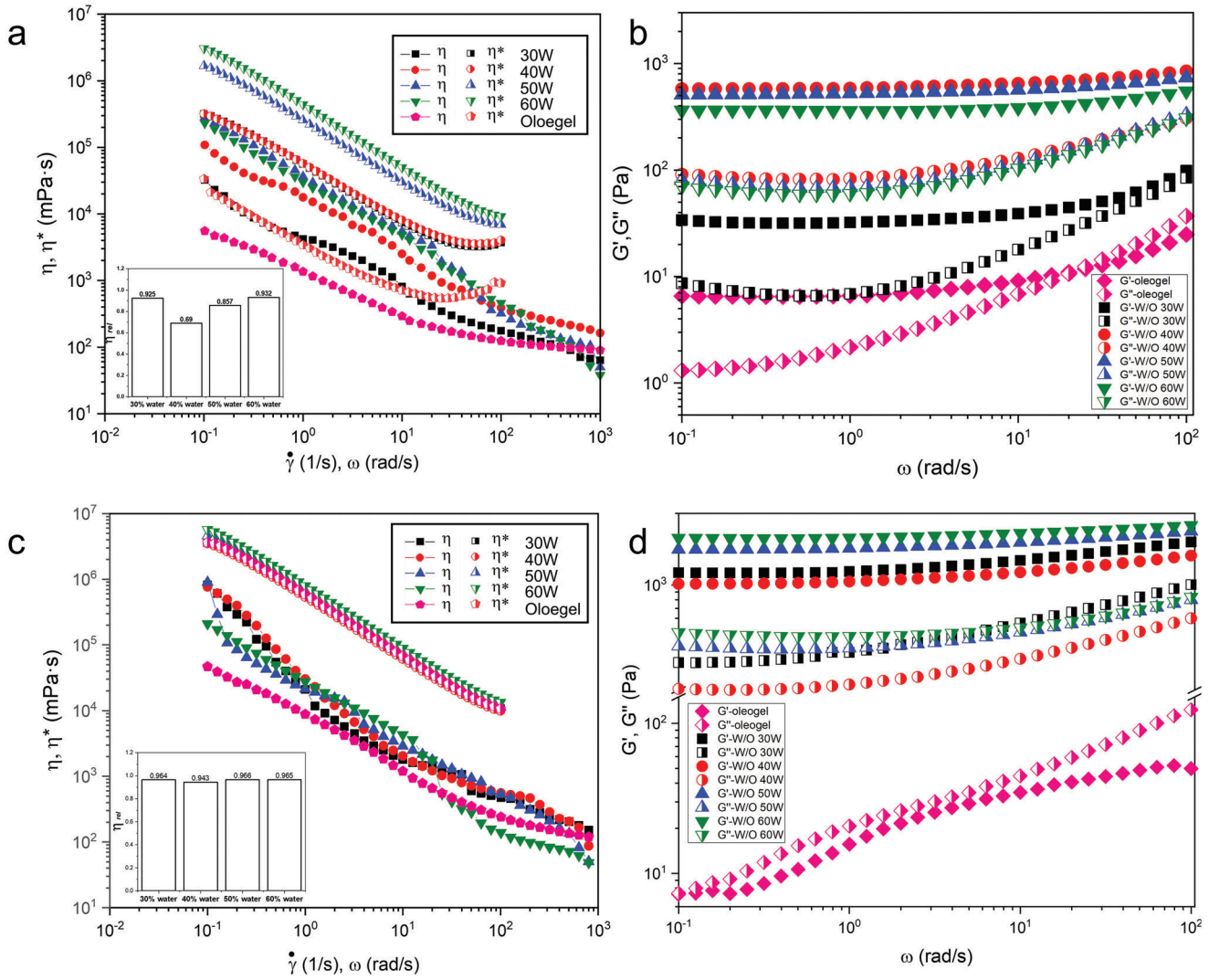

Figure 9. Rheological properties of oleogels and W/O emulsions containing different volume fractions of water. The effect of the water content in freshly prepared W/O emulsions on the apparent viscosity (a), and modulus (b). The apparent viscosity (η) and complex viscosity (η^*) of freshly prepared emulsions were measured after 10 min of preparation in a modular compact rheometer MCR 302 stress-controlled at shear rates ranging from 0.1 to 1000 s^{-1}. Viscosity (c) and sweep frequency (d) tests were carried out to measure the viscoelastic properties of the oleogel containing 15% (v/v) CB crystals, i.e., (15CBolg) and the corresponding W/O emulsions containing various volume fractions of water (30–60% (v/v)) after 1 month of storage to measure the effect of CB crystals in the emulsions. The emulsions were stored at 23 °C for 4 weeks. Superimposition of the shear viscosity (η) and complex viscosity (η^*) as a function of shear rate ($\dot{\gamma}$) and angular frequency (ω) is shown in the plot of viscosity as insets for both fresh and 1-month storage emulsions (a,c), respectively. The bar graph illustrates the relative deviation values of the Cox-Merz rule for fresh and 1-month aged emulsions. The data shows the means of three measurements on triplicate samples (n = 3 × 3).

of emulsions with 50 and 60% (v/v) of water, the low viscosity at higher shear rates is related to the breakup of the emulsions.

Considering the gel-like visual behavior of these emulsions before and after storage (Figures 3 and 7, and Figure S5b, Supporting Information), small oscillatory rheology was performed. Both 15CBolg and emulsions with 30–60% (v/v) water showed viscoelastic properties with a predominant elastic behavior, which is also linked to the interactions between droplets and CB crystals in the oleogel. As shown in Figure 9b, the storage (G') and loss (G'') modulus were lower for the oleogels and the emulsions with 30% (v/v) water than for emulsions with 40–60% (v/v) of water by nearly two orders of magnitude. The emulsions demonstrated a dominant elastic behavior across all the frequencies, while the 15CBolg presented a disruption of its structure at higher frequency (25.1 rad s^{-1}) with the G'' modulus exceeding the G' modulus. This observation suggests that this oleogel exhibits a predominant viscous behavior in such high frequency. This indicates that the water droplets acted as the so-called "active fillers"[50] and reinforced the crystal network. Hence, the fat crystals at the interface and those in the bulk phase, together with the content of water determined how the material deforms and breaks.

The size of the CB crystals might play a relevant role in the rheological properties of Pickering emulsions, as the interactions

among the crystals and water droplets over time may evolve. As discussed before, with time, the size of CB crystals increased due to Ostwald ripening and also the strength of the crystalline network in the bulk phase increased during storage. Hence, it is not surprising that the emulsions containing 30–40% (v/v) of water showed overlapping behavior to that of the oleogels except at higher water contents (50–60% (v/v) water) (Figure 9c). Of more importance, the rigidity of W/O emulsions containing 30–60% (v/v) was restored with a water dose-dependent manner even after a month of storage (Figure 9d) highlighting that the Pickering water droplets acting as active fillers reinforced the fat continuous matrix permanently without any syneresis during the storage period.

The Cox–Merz rule, an empirical relation, states that the complex viscosity (η^*) is approximately equal to its steady shear viscosity (η) of an emulsion when the frequency and shear rate are equal ($\eta(\dot{\gamma}) = \eta^*(\omega)$). Figure 9a depicts the η and η^* for all the emulsions before and after storage for 1 month.[51] As has been found in previous studies for emulsions, the values of the η^* are higher than the η[52–54] The Cox-Merz however has been observed to fail in solution where the elastic contribution has a significant effect, leading to deviations between η and η^*.[55,53] The results obtained in the present study confirm that the higher the elasticity (indicated by longer relaxation times) the departure from the rule becomes more noticeable. For instance, the deviation from the Cox-Merz rule in the CB oleogel is comparatively smaller as compared to those in the emulsions. The viscoelastic results (Figure 9b) confirm that the CB oleogels exhibit a lower degree of elastic behavior in comparison to the emulsions.[54] The observations of CB oleogels are consistent with previous findings on concentrated dispersions of polymers.[55,56]

Often a modified version of the Cox-Merz rule has been suggested,[53] where the η^* is expressed as a function of the product of strain rate ($\dot{\gamma}$) and frequency (ω). Although certain emulsions show a correlation between both these viscosities with this modification,[53] the W/O emulsions in this study do not show such overlaps (Figure S6, Supporting Information). This suggests that the internal structure provided by the water and the CB crystals has a significant influence on the rheological behavior. The deviation from the Cox-Merz rule in CB-stabilized emulsions might be attributed to the presence of the network between the water droplets and the crystals surrounding the water droplets as observed in the CLSM images (Figure 4). The relative deviation of the Cox-Merz rule (η_{rel}) can be calculated independently of the frequency or shear rate using the followed equation:

$$\eta_{rel} = \left. \frac{\eta^* - \eta}{\eta^*} \right|_{\dot{\gamma}=\omega} \quad (2)$$

The η_{rel} of the Cox–Merz rule provides insights into the extent to which a material deviates from the expected relationship between η and η^*, indicating the complexity in the emulsion's rheological behavior. Based on the findings from Figure 9a, it can be observed that all fresh emulsions exhibited significantly high ($p < 0.05$) values of η_{rel} ranging from 0.85 to 0.93, except for the emulsion containing 40 W, which presented the lower value (0.69). A higher relative deviation of the Cox–Merz rule suggests a greater departure from the expected relationship between η and η^*. This indicates that the material's response to steady shear is enough to disrupt the structured inter- and intramolecular associations.[51,57] In the case of the fresh emulsions, the result from Figure 9a did not show a consistent trend with the increasing water content. This inconsistency could be attributed to the presence of CB crystals, which require more time to reach an equilibrium state at the interface and fully contribute to the rheological properties of the emulsions.

Noteworthy, that the fat crystals have the tendency to grow over time due to the Ostwald ripening phenomenon[41,58,59] This means, that the network of crystals can undergo continuous evolution and growth for an extended period, lasting several weeks or months, until it eventually reaches a state of equilibrium. Thus, the rheological properties of the emulsions are also expected to evolve. The η_{rel} values for emulsions storage for one month (Figure 9c) did not show a significant difference between all emulsions, thus confirming that the crystal evolution during storage plays a crucial role in the rheology of the CB-stabilized emulsions. Of more importance, the unusual rigidity of W/O emulsions containing 30–60% (v/v) was restored with a water dose-dependent manner even after a month of storage (Figure 9d) highlighting that the Pickering water droplets acting as active fillers reinforced the fat continuous matrix permanently without any syneresis during the storage period. The CLSM images (comparing Figure 4 with 8) clearly demonstrate the evolution of the crystals with time, with an increase in the size of crystals, supporting the higher apparent η and η^* (Figure 9a,c), enhanced shear-thinning behavior and enhanced rigidity (Figure 9b,d). Also, the water content of the emulsions contributed significantly to the final mechanical properties after preparation and as a function of storage. In summary, the novel findings from this study show the subtle balance between the concentration of CB crystals and water content as well as processing conditions use of HOSO, time, and temperature of crystallization), which can be exploited to generate stable Pickering emulsions with a high water content that also show tunable rigidity. The results for both fresh and storage emulsions the solid-like behavior increases proportionally to the water content.

3. Conclusions

This study demonstrated that CB crystals can stabilize emulsifier-free W/O emulsions by a combination of Pickering (interfacial) and network stabilization. The fat crystals generated by oleogelation of CB with HOSO offer particles with unique wettability that protected water droplets' stability against coalescence and phase separation during the emulsification as well as during long-term storage. The crystalline network stabilization further enhanced the stability by the interlocking of the water droplets. The temperature, time of crystallization (affecting SFC, size, and shape of the crystals), and the concentration of CB in the oleogels were the key factors to generate ultrastable W/O emulsions, and more importantly to incorporate high concentrations of water, up to 60 (v/v)%. The rheological properties of the W/O emulsions were modified by altering the water content and the concentration of CB crystals, as the interactions of the water droplets and the crystalline network determine the final rigidity of these fat continuous emulsions. Strikingly, increasing the water content increased the strength of these interactions, with water droplets acting as "active fillers" and providing higher viscosity values, and a

predominant elastic behavior. Nonetheless, Ostwald ripening of the CB crystals during storage further strengthened the elasticity of the emulsions. Thus, these studies pave the way forward towards designing soft elastic fat continuous materials with tunable rheological properties, containing high concentration of water by modifying the water content, CB concentration in the oil, temperature, and time of processing affecting SFC for use in food, pharmaceutical and personal care industries.

4. Experimental Section

Materials: Polyglycerol polyricinoleate (PGPR) was kindly donated by Palsgaard, Denmark. Refined, bleached, and deodorized cocoa butter (CB) and high oleic sunflower oil (HOSO) were obtained from Cargill (UK). The nominal composition of the fatty acids present in CB is: 36% stearic acid, 34% oleic acid, 26% palmitic acid, 2.7% linoleic acid, and 0.9% arachidic acid by weight.[8] Meanwhile, HOSO contains 86% oleic acid, 5% stearic acid, 3% linoleic acid, 3% palmitic acid, 1.5% behenic acid, and 0.7% arachidic acid by weight.[8] Sodium phosphate monobasic monohydrate, sodium phosphate dibasic anhydrous, and hydroxyl chloride were purchased from Thermo Fisher Scientific Loughborough, UK. Sodium azide (0.02%) was obtained from Sigma Aldrich (USA) and used as an antibacterial agent.

Preparation of Oleogels: In order to produce the fat crystals to stabilize the water-oil emulsions, an oleogel was first generated using a combination of CB and high oleic sunflower oil (HOSO) by subjecting this mixture to a controlled crystallization process. First, the CB was melted in a water bath at 80 °C for at least 20 min. Then CB was mixed with HOSO using a stirring hot plate for 5 min. For convenience, CB/HOSO oleogels will be referred to as CB oleogels (CBolgs), taking into account that CB fat is the key gelator of the liquid HOSO. Approximately, 100 mL of CB/HOSO blend was added to a jacketed vessel connected to a Huber Ministat 125 thermostat (Huber Germany) for temperature control.

During the crystallization process, the samples were continuously sheared at 200 rpm using a magnetic stirring plate, whilst the temperature was being monitored continuously using a PT-100 temperature sensor, which was located inside the vessel. The light absorbance and transmittance are approximate indications of the magnitude of dispersed materials present in a liquid suspension.[8] Thus, these parameters were monitored to examine the crystallization process (see Figure S1, Supporting Information). Both these aforementioned parameters were measured by a Control 4000 turbidity meter equipment (Optek, Germany) fitted with an ASD12-N absorption probe.

Different cooling rates of CB oleogels have been studied previously[8] Therefore, experiments were performed following the previously reported methodology with slight modifications. Once the solid CB is melted and mixed efficiently, the blend was maintained at 55 °C for 15 min initially in order to equilibrate the temperature. Then the jacket temperature was reduced from 55 °C to 37 °C at −1 °C min^{-1} cooling rate, followed by reduction to 0 °C at a cooling rate of −0.75 °C min^{-1} and maintained at this temperature for 90 min. The oleogels formed were then heated to 23 °C, which is the limiting tempering temperature to preserve an acceptable amount of CB crystals for the emulsion formation. Finally, the oleogels were maintained at 23 °C for 12 h before being used for emulsion preparation.

To investigate the structure of CB crystals, a blend of CB/HOSO with different CB concentration (10%, 15%, and 20%, V/V) were used and the same blend was subjected to different tempering conditions (23 °C and 17 °C). All samples were maintained in the vessel for the same studied temperature and evaluated at 12 h and 4 days to ensure uniform conditions across all the samples.

Preparation of W/O Emulsion Preparation: The aforementioned oleogels containing fat crystals were used as Pickering particles to stabilize water-in-oil (W/O) emulsions (30–60% (v/v) water). Three different CB concentrations (10%, 15%, and 20% (v/v)) were used to stabilize the water droplet without the addition of any surfactant. It is worth noting that the crystallization process of the CB crystals and henceforth mentioning profile was affected by the presence of triacrylglycerols of the HOSO, the latter reducing the characteristic melting point of the pure CB. Therefore, the fat crystals formed in the oleogel and then located at the interface or continuous of the water droplets might not be pure CB crystals. As the CB crystals are temperature sensitive, the emulsion preparation was performed in a vessel connected to a Tamson low-temperature circulator (TLC2, PMT, Zoetermeer-Holland) filled with water, to maintain the temperature at 23 °C during the emulsification process. The water phase (phosphate buffer 15 mM at pH 7.0) used to form the emulsions was cooled to 4 °C before the emulsification process to counteract any temperature increase during the homogenization process. The emulsions were prepared by mixing the cold water phase with the corresponding volume fraction of CB oleogels, followed by emulsification with a rotor-stator emulsifier (Ultra-Turrax S25N-18G, IKA, Staufen) at 24, 000 rpm for 40 s. Emulsions were also prepared using PGPR to act as a control surfactant-stabilized emulsion. All samples were stored immediately at 23 °C in a temperature-controlled cabinet.

Polarized Light Microscopy (PLM): The fat crystals present in the oleogels were observed with a Leitz Dialux 22 polarized microscope (Leica, Germany). In order to maintain the temperature at 23 °C or 17 °C, depending on the test, the normal stage on the PLM was removed and a Cambridge Shearing system stage (CSS450, Linkam Scientific Instrument Ltd, UK) was placed instead. The CSS450 allows to control the desired temperature by heating or cooling the system with liquid nitrogen. A small amount of the CB/HOSO oleogel was placed in the quartz plate and the upper quartz plate was positioned with a micron accuracy at a distance from the bottom plate of 100 µm. The distance can be controlled with the dedicated software from 0 to 2500 µm. The PLM was fitted with a Canon DLSR camera. The digital images were acquired with 50× magnification. The images acquired were processed by ImageJ, version 1.52p (National Institute of Health, Bethesda, USA).

Measurement of Water Droplet Size: Nearly, 0.5 g of the emulsions were diluted in 9.5 g of HOSO with 4.0 wt% of PGPR and heated at 30 °C.[60] One droplet of the diluted sample was placed in the quartz plate of the CSS4550, and the gap was fixed to 100 µm, to allow spreading of the water droplets. At least a hundred different images of the morphology of the water droplets were obtained at different points of the rotating bottom plate, so the images were well representative of the emulsions. The measurement of the droplet size was performed by using image analysis using bright field optical microscopy. The emulsions were imaged after their preparation and every week during one month of storage at 23 °C. The droplet size was also measured after 7 months of storage at the controlled temperature (23 °C). The images were processed with a MATLAB R2019a code (MathWorks, USA) by using the *Imfindcircles* function, which measures the radius of the spherical objects in the image. The "*imfindcircles*" algorithm of Mathlab that uses a circular Hough transform to find circles. This algorithm has two filters, the first one is the Sensitivity factor (within a range of [0, 1]), which allows the detection of more circular objects—the higher the value, the weaker the criteria for the detection of partially undefined circles, but errors increase as well. The second filter is the Edge gradient threshold which sets the grayscale gradient threshold for determining valid edge pixels with a valid range [0, 1], with a low detection of weak edges when the Threshold has a higher value. Thus, the "*infindcirles*" algorithm was run for each image, its quality was enhanced by using filters (Stretchlim, mean_image, Ifilled (Holes), and strel) that allowed defining of the edges of the spherical droplets. Due to the resolution (0.7 µm) of the objective used (50x/0.45), two different sets of optimizing filter values were used depending on the range of diameters: (a) for drops in an interval of 0.2-0.5 µm, a sensitivity of 0.70 and Edge Threshold of 0.1 were used, and (b) for drops between 0.6 and 100 µm, 0.94, and 0.1, respectively, were used. This was done to avoid the determination of the small dark circles which can give to wrong droplet size measurements. The droplet diameter was fitted to a 3-parameter lognormal distribution as this showed a better fitting according to the probability plots and the threshold parameter of the distribution, which had a lower value than that of the distribution.

Confocal Laser Scanning Microscopy (CLSM): The morphology of the W/O emulsions was characterized using a Zeiss LSM 880inverted micro-

scope (Carl Zeiss MicroImaging GmbH, Jena, Germany). Approximately, 10 µL of a mix of Nile Red (0.002 mg/mL in dimethyl sulfoxide, final concentration) and Nile blue (0.1 mg/mL in MilliQ water, final concentration) were added to 1 g of emulsions. Emulsions after their preparation and after one month of storage at 23 °C were fluorescently dyed with the above mixture. The stained emulsions were placed into a concave confocal microscope slide and covered with a glass coverslip and observed in the microscope after around 10 min. The images were acquired using an oil immersion 63× lens and the pinhole was kept at 1 Air Unit to filter out the majority of light scattering. The wavelength used to excite Nile Red was 488 nm, while Nile blue was 625 nm.

Cryogenic Scanning Electron Microscopy (CryoSEM): Micrographs of W/O emulsions (30% (v/v water) stabilized with 20% (v/v) of CB crystals were acquired using a Helios G4 CX DualBean scanning electron microscope (FEI, USA) coupled with a PP3010T Cryo-FIG/SEM preparation system (Quorum Technologies, UK) The precooled rivet holder was filled with the sample, which was frozen with liquid nitrogen. The frozen sample was inserted in the preparation sample chamber and kept at −145 °C under vacuum ($<10^{-7}$ mbar), and then it was fractured with a cooled sharp knife and sublimed at −90 °C. Then the sample was cooled again at −145 °C and sputtered with iridium (10 mA for 30 s). Finally, the sample was transferred inside the microscope chamber. Images were acquired at 2 kV accelerating voltage and 0.10 nA beam current.

X-Ray Scattering: Small-angle X-ray scattering (SAXS) and wide-angle X-ray scattering (WAXS) measurements were performed on oleogels and corresponding W/O emulsions containing 20% (v/v) CB with a SAXSpace instrument (Anton Paar GmbH, Austria). The instrument is equipped with a Cu anode ($\lambda = 0.154$ nm). The temperature was set to 23 °C, which is controlled by a TCstage 150 Peltier element (Anton Paar, Austria). The SAXS and WAXS measurements were performed at a sample-detector distance of 130 mm. The 1D scattering patterns were recorded with a Mythen microstrip X-ray detector (Dectris Ltd., Baden, Switzerland).

Due to the high viscosity of the 20% (v/v) CB oleogels and the corresponding fat crystal-stabilized emulsions, the samples were loaded into a paste cell with X-ray transparent Kapton windows. The HOSO and phosphate buffer were injected into quartz disposable capillaries (Capillary Tube Supplies Ltd., Cornwall, UK) with an outside diameter of 1.5 mm. The capillaries were subsequently sealed with wax. SAXSTreat software (Anton Paar GmbH, Graz, Austria) was used to set to zero the position of the primary beam in all the patterns. The recorded scattering patterns were normalized for their transmission by using the SAXSQuant software (Anton Paar GmbH, Graz, Austria). From the normalized CB oleogel pattern, the empty paste cell and HOSO scattering were subtracted, while for the emulsion pattern, the empty paste cell and the buffer scattering were subtracted. The empty capillary scattering was subtracted from the HOSO. The peak fit analysis was carried out in OriginPro 2019b.

The area per chain in the given oblique sub-cell, concerning the Miller indexes (10), (11), and (−11) was calculated applying the following equation (2):

$$A_C = \frac{2 \cdot d_{10}^2 d_{-11}^2 d_{01}^2}{\sqrt{(d_{10}d_{-11} + d_{-11}d_{01} + d_{01}d_{10})\,(-d_{10}d_{-11} + d_{-11}d_{01} + d_{01}d_{10})\,(d_{10}d_{-11} - d_{-11}d_{01} + d_{01}d_{10})\,(d_{10}d_{-11} + d_{-11}d_{01} - d_{01}d_{10})}} \quad (3)$$

Note, the determination of the area per chain can was solved by applying Heron's formula.[61]

Differential Scanning Calorimetry (DSC): Samples of the 10, 15, and 20 CB were weighted and sealed hermetically in aluminum pans (Tzero, TA Instruments, Elstree, UK). Around 0.012 ± 0.002 g was used to investigate the melting behavior of the CB and oleogel samples at different temperatures (17 °C and 23 °C). The measurements were performed in a DSC Q-20 instrument (TA Instrument, Elstree, UK). The samples were melted from 23 to 55 °C at a heating rate of 5 °C min^{-1}. TA Universal Analysis 2000 software (version 4.5A) was used to obtain the endpoint for the CB oleogels melting.

Rheology: Flow behavior of the oleogels and the corresponding W/O emulsions stabilized by fat crystals with different water contents as well as W/O emulsions stabilized by PGPR were performed in a modular compact rheometer MCR 302 stress-controlled (Anton Paar, Austria) at shear rates ranging from 0.1 to 1000 s^{-1}. The emulsion samples were examined 10 min after their preparation and after a storage period of 4 weeks. A plate-plate geometry (50 mm) with a gap of 1 mm was used for all the measurements. The apparent viscosity was measured at 23 °C. Samples were left on the plate for 1 min to achieve a steady state, and then the viscosity test was performed. The linear viscoelastic region (LVR) of the samples was determined by strain sweep (0.01-100%) at a frequency of 1 Hz at 23 °C. The dynamic yield stress was determined as the stress level at which a deviation from linearity was observed (0.5% strain). Frequency sweep tests were performed with 15CB oleogels and the corresponding W/O emulsions (30-60% (v/v) water) containing fat crystals (15CB) at an angular frequency ranging from 0.1 to 1000 $rads^{-1}$ at 0.1% strain after preparation and after one month of storage. Some experiments were repeated with a serrated plate (profiled 1 ×0.5 mm) to check for slippage and data showed no significant difference to those obtained with the non-serrated parallel plate geometry.

Statistical Analysis: Three independent measurements were carried out at least in triplicate experiments ($n = 3 \times 3$) and data are represented as means and standard deviations. One-way analysis of variance with follow-up Tukey's multiple comparisons test was employed to determine significant differences ($p < 0.05$) using the software Minitab.

Supporting Information

Supporting Information is available from the Wiley Online Library or from the author.

Acknowledgements

E.T.-G. acknowledges financial support from the Mexican National Council of Science and Technology (CONACyT) for the award of an Academic Scholarship for her Ph.D. studies. E.S. has received funding for this collaboration from the European Research Council (ERC) under the European Union's Horizon 2020 research and innovation program (grant agreement No 949229).

Conflict of Interest

The authors declare no conflict of interest.

Data Availability Statement

The data that support the findings of this study are available from the corresponding author upon reasonable request.

Keywords

cocoa butter crystals, scattering, oleogels, Pickering particles, rheology, storage

Received: March 5, 2023
Revised: June 22, 2023
Published online: July 23, 2023

[1] V. Nelis, A. Declerck, L. Vermeir, M. Balcaen, K. Dewettinck, P. Van der Meeren, *Magn. Reson. Chem.* **2019**, *57*, 707.
[2] V. Patel, J. Andrade, D. Rousseau, *LWT* **2021**, *149*, 111802.
[3] R. Rafanan, D. Rousseau, *J. Food Eng.* **2019**, *244*, 192.
[4] S. Ghosh, D. Rousseau, *Curr. Opin. Colloid Interface Sci.* **2011**, *16*, 421.
[5] M. Zembyla, B. S. Murray, A. Sarkar, *Trends Food Sci. Technol.* **2020**, *104*, 49.
[6] S. Ghosh, T. Tran, D. Rousseau, *Langmuir* **2011**, *27*, 6589.
[7] A. P. Ribeiro, M. H. Masuchi, E. K. Miyasaki, M. A. Domingues, V. L. Stroppa, G. M. de Oliveira, T. G. Kieckbusch, *J. Food Sci. Technol.* **2015**, *52*, 3925.
[8] L. Metilli, A. Lazidis, M. Francis, S. Marty-Terrade, J. Ray, E. Simone, *Cryst. Growth Des.* **2021**, *21*, 1562.
[9] S. S. Sagiri, K. J. Rao, in *Biopolymer-Based Formulations* (Eds: K. Pal, I. Banerjee, P. Sarkar, D. Kim, W.-P. Deng, N. K. Dubey, K. Majumder), Elsevier, Cham, Switzerland **2020**, pp. 513.
[10] X. Hong, Q. Zhao, Y. Liu, J. Li, *Crit. Rev. Food Sci. Nutr.* **2021**, 1406.
[11] E. Tenorio-Garcia, A. Araiza-Calahorra, E. Simone, A. Sarkar, *Food Hydrocolloids* **2022**, *128*, 107601.
[12] S. Tao, H. Jiang, R. Wang, C. Yang, Y. Li, T. Ngai, *Chem. Commun.* **2020**, *56*, 14011.
[13] B. Pang, H. Liu, P. Liu, X. Peng, K. Zhang, *J. Colloid Interface Sci.* **2018**, *513*, 629.
[14] M. Zembyla, A. Lazidis, B. S. Murray, A. Sarkar, *Langmuir* **2019**, *35*, 13078.
[15] M. Zembyla, B. S. Murray, A. Sarkar, *Langmuir* **2018**, *34*, 10001.
[16] M. Zembyla, B. S. Murray, S. J. Radford, A. Sarkar, *J. Colloid Interface Sci.* **2019**, *548*, 88.
[17] H. Jiang, X. Hu, W. Jiang, X. Guan, Y. Li, T. Ngai, *Langmuir* **2022**, *38*, 12273.
[18] A. R. Patel, D. Schatteman, W. H. De Vos, A. Lesaffer, K. Dewettinck, *J. Colloid Interface Sci.* **2013**, *411*, 114.
[19] D. O. García-González, B. Yánez-Soto, E. Dibildox-Alvarado, J. d. J. Ornelas-Paz, J. D. Pérez-Martínez, *LWT* **2021**, *146*, 111405.
[20] J. Yang, C. Qiu, G. Li, W. J. Lee, C. P. Tan, O. M. Lai, Y. Wang, *Food Chem.* **2020**, *327*, 127014.
[21] S. Watanabe, S. Yoshikawa, K. Sato, *Food Chem.* **2021**, 339.
[22] V. A. Fernandes, A. J. Müller, A. J. Sandoval, *J. Food Eng.* **2013**, *116*, 97.
[23] A. G. Marangoni, S. E. McGauley, *Cryst. Growth Des.* **2003**, *3*, 95.
[24] J. Chen, S. M. Ghazani, J. A. Stobbs, A. G. Marangoni, *Nat. Commun.* **2021**, *12*, 5018.
[25] a) J. E. Norton, P. J. Fryer, J. Parkinson, P. W. Cox, *J. Food Eng.* **2009**, *95*, 172; b) V. Prosapio, I. T. Norton, *J. Food Eng.* **2019**, *261*, 172.
[26] A. Sullo, M. Arellano, I. T. Norton, *J. Food Eng.* **2014**, *142*, 100.
[27] L. Metilli, L. Morris, A. Lazidis, S. Marty-Terrade, M. Holmes, M. Povey, E. Simone, *J. Food Eng.* **2022**, *335*, 111192.
[28] J. Farmani, *J. Food Measure. Character.* **2015**, *9*, 281.
[29] A. G. Marangoni, N. Acevedo, F. Maleky, E. Co, F. Peyronel, G. Mazzanti, B. Quinn, D. Pink, *Soft Matter* **2012**, *8*, 1275.
[30] T. Tran, D. Rousseau, *Food Res Int* **2016**, *81*, 157.
[31] D. Pérez-Martínez, C. Alvarez-Salas, M. Charó-Alonso, E. Dibildox-Alvarado, J. F. Toro-Vazquez, *Food Res Int* **2007**, *40*, 47.
[32] S. Sonwai, M. R. Mackley, **2006**, *83*, 583.
[33] D. Pérez-Martínez, C. Alvarez-Salas, J. A. Morales-Rueda, J. F. Toro-Vazquez, M. Charó-Alonso, E. Dibildox-Alvarado, **2005**, *82*, 471.
[34] G. I. Taylor, *R. Soc. Lond. Ser. A* **1939**, 501.
[35] a) J. A. Pathak, M. C. Davis, S. D. Hudson, K. B. Migler, *J. Colloid Interface Sci.* **2002**, *255*, 391; b) A. Vananroye, P. V. Puyvelde, P. Moldenaers, *Langmuir* **2006**, *22*, 391.
[36] H. Grace, *Chem. Eng. Commun.* **1982**, *14*, 225.
[37] R. Bruijn, *Doctoral dissertation*, Techniche Universiteit Eindhoven, **1989**.
[38] J. Cruz-Mena, F. Serrania, B. Mena, *Progress and Trends in Rheology II* **1988**, *26*, 262.
[39] M. El-Aooiti, A. de Vries, D. Rousseau, *J. Colloid Interface Sci.* **2020**, *580*, 630.
[40] A. Sarkar, E. Dickinson, *Curr. Opin. Colloid Interface Sci.* **2020**, *49*, 69.
[41] M. Adam-Berret, M. Boulard, A. Riaublanc, F. Mariette, *J. Agric. Food Chem.* **2011**, *59*, 1767.
[42] R. Campos, M. Ollivon, A. G. Marangoni, *Cryst. Growth Des.* **2010**, *10*, 205.
[43] D. M. Small, *J. Lipid Res.* **1984**, *25*, 1490.
[44] S. H. J. Idziak, in *Structure-Function Analysis of Edible Fats*, 2nd ed. (Ed: A. G. Marangoni), AOCS Press, Urbana, IL **2018**, pp. 73.
[45] A. Sarkar, P.-A. Golay, S. Acquistapace, B. D. Craft, *Int. J. Food Sci. Technol.* **2015**, *50*, 666.
[46] L. Metilli, M. Storm, S. Marathe, A. Lazidis, S. Marty-Terrade, E. Simone, *Langmuir* **2022**, *38*, 1638.
[47] P. L. Fuhrmann, S. Breunig, G. Sala, L. Sagis, M. Stieger, E. Scholten, *J. Colloid Interface Sci.* **2022**, *607*, 389.
[48] M. Zembyla, A. Lazidis, B. S. Murray, A. Sarkar, *J. Food Eng.* **2020**, *281*, 109991.
[49] C. Liu, M. Li, R. Han, J. Li, C. Liu, *J. Dispersion Sci. Technol.* **2016**, *37*, 333.
[50] O. Torres, E. Andablo-Reyes, B. S. Murray, A. Sarkar, *ACS Appl. Mater. Interfaces* **2018**, *10*, 26893.
[51] A. P. Batista, A. Raymundo, I. Sousa, J. Empis, J. M. Franco, *Recent Adv. Food Sci.* **2006**, *1*, 216.
[52] D. Doraiswamy, A. N. Mujumdar, I. Tsao, A. N. Beris, S. C. Danforth, A. B. Metzner, *Journal of Rheology* **1991**, *35*, 647.
[53] W. J. Han, H. J. Choi, Y. Seo, *Smart Mater. Struct.* **2020**, *29*, 085022.
[54] M. Anvari, H. S. Joyner, *Food Res Int* **2017**, *102*, 1.
[55] N. Calero, J. Muñoz, P. Ramírez, A. Guerrero, *Food Hydrocolloids* **2010**, *24*, 659.
[56] J. Muñoz, F. Rincón, M. Carmen Alfaro, I. Zapata, J. de la Fuente, O. Beltrán, G. León de Pinto, *Carbohydr. Polym.* **2007**, *70*, 198.
[57] M. A. Riscardo, J. E. Moros, J. M. Franco, C. Gallegos, *Eur. Food Res. Technol.* **2005**, *220*, 380.
[58] C. Delbaere, D. Van de Walle, F. Depypere, X. Gellynck, K. Dewettinck, *Eur. J. Lipid Sci. Technol.* **2016**, *118*, 1800.
[59] E. O. Afoakwa, A. Paterson, M. Fowler, J. Vieira, *J. Food Eng.* **2009**, *91*, 571.
[60] L. Goibier, C. Pillement, J. Monteil, C. Faure, F. Leal-Calderon, *Colloids Surf. A* **2020**, *590*, 124492.
[61] D. W. Mitchell, *Math. Gazette* **2005**, *89*, 494.